RF Analysis of Fruit and Vegetables using Equivalent Circuits Deduced from S-parameters

Koyu Chinen[1*], Shoko Nakamono[1], Ichiko Kinjo[2]
[1]GLEX, Japan,
Email: koyu.chinen@nifty.com
[2]National Institute of Technology, Okinawa College, Japan,
Email: ichi@okinawa-ct.ac.jp
[*] Corresponding author

Abstract: **We deduced equivalent circuits of the electrical properties of five fruit and eight vegetable samples from the S-parameters. The S-parameters were measured at a frequency range from 1 MHz to 100 MHz using a portable VNA and a tiny three-pin SMA probe. Admittance values calculated from the S-parameters were plotted on the admittance Smith chart, and the equivalent circuits with four parallel sub-circuits were synthesized by curve fitting. The admittance curves for the fruit and vegetable samples have two parts with different lengths split at a frequency of about 30 MHz. The admittance in the low-frequency range was determined mainly by two large capacitive and two small resistive elements of the equivalent circuit related to the plant cell wall and membrane. When the plant cell wall and membrane were decomposed by grating and 30μm-filtering, the specific part of the admittance curve was eliminated, and the admittance value increased. The measured and calculated admittance curves were in good agreement. About 30 samples of plant cultivars were classified as fruit and vegetables according to four criteria deduced from the RF analysis. S-parameter spectroscopy (SPS) is an effective analytical method for evaluating the electrical properties of plant tissues.**

Keywords: **S-parameter, SPS, fruits and vegetables, equivalent circuit, Smith-chart.**

I. INTRODUCTION

Degradation and changes in taste, freshness, and maturity are of great concern in agricultural products. Therefore, electrochemical impedance spectroscopy (EIS) has been widely used to assess and evaluate changes in the quality of fruits and vegetables [1-4]. Since EIS is a non-destructive, simple, and fast measurement technique, it has been applied to investigate the relationship between electrical properties and quality of fruits and vegetables such as apples [5-12], bananas [10,12,13], orange [14], papaya [15], mango [16], melon [17], tomato [18,19], potato [20,21], and carrot [22]. The EIS measurement system is generally configured with an impedance analyzer or an LCR meter connected with two or four-port electrodes and an open-ended coaxial probe to measure the impedance of the plants. Therefore, low-frequency signals and high-input-impedance have generally been used to measure the high-impedance of biological tissues, and it has also been difficult to reduce the mechanical size of the electrode and the contact resistance between the electrode and the high-impedance skin of the biomaterial [23]. The measured complex dielectric constants were plotted on Nyquist grids (Cole-Cole plot) to analyze the dielectric properties of the biological tissue.

In this work, we used a 50Ω impedance matched vector network analyzer (VNA) and a tiny SMA (sub-miniature type A) probe to measure the scattering (S)-parameters and to deduce equivalent circuits. A similar measurement method was used to analyze the solutions of different NaCl concentrations [24]. In this paper, we discuss the validity of the deduced equivalent circuits, the electrical properties of fruits and vegetables, and the correlation between the parts of the plant cell and the equivalent circuit by using S-parameter spectroscopy (SPS). The S-parameter measurement and analysis involve the modulation and measurement of small amplitude signals. The fruits and vegetables to be measured are treated as passive linear devices, and their equivalent circuit is a passive circuit without current sources.

II. EXPERIMENTAL SETUP EQUIVALENT CIRCUITS DEDUCED FOR FRUITS AND VEGETABLES

We measured S-parameters at 100 points in the frequency range from 1 MHz to 100 MHz using the vector network analyzer (VNA) with two 50 Ω impedance ports, 20 cm long 50 Ω coaxial cables, and 50 Ω SMA probes. A portable and inexpensive VNA (55 mm × 90 mm × 25 mm) [25] was used as the VNA. We can easily carry the VNA on-site, such as a farm or workshop. Figure 1 shows an experimental setup configured with the VNA and the tiny SMA probe. The measurement calibration for the setup was performed using SOLT (short, open, load, thorough) - SMA connectors, and the validity of the calibration was confirmed by measuring a 1200Ω-SMD (surface mount device, 1608 in size) resistor soldered between the signal and ground pins of the SMA probe. The SMA probe has a central signal pin (Au-plated Cu, 4 mm × ϕ 0.8 mm) surrounded by polytetrafluoroethylene (PTFE) and two ground pins (Au-plated brass, 4 mm × ϕ 0.8 mm) on either side. The number of ground pins was determined by experimental evaluation of electrical sensitivity and ease of insertion using zero to four ground pin probes. This optimized design of the SMA probe ensured that we could easily insert it into most fruits and vegetables and even into the grain of corn and the uneven surface of bitter melon.

In general, the plant cell consists of different materials, as shown in Fig. 2, and the nucleus and vacuole are surrounded by a membrane and wall. The vacuole contains ionized

materials, such as Na^+, Ca^+, K^+, Cl^-, $HPO2^-$, etc., and polar molecules of the solvent, such as H_2O. These ions and polar molecules are moved, rotated, and vibrated by applied high-frequency electrical signals. Therefore, we can measure the electrical signals reflected from these ionic materials, and the measurement of the S-parameter enables us to collect different electrical information from biological tissues.

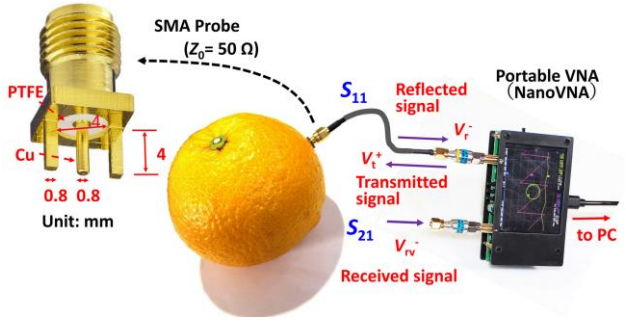

Fig. 1. Configuration of a setup using a portable VNA and tiny SMA probe to measure the S-parameters for fruit and vegetables.

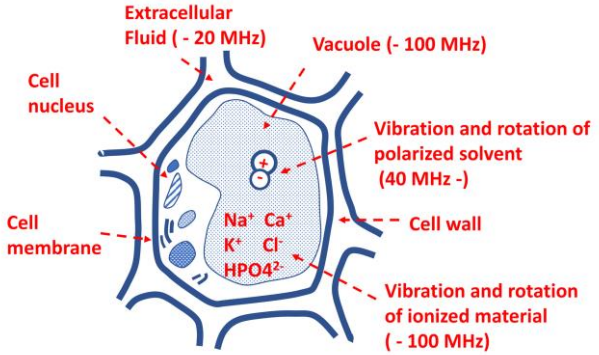

Fig. 2. Relationship between electrical conductance and parts of the plant cell configuration.

The values of the S-parameters measured were analyzed using an RF circuit simulator of AWR-MWO [26], and we were able to deduce the equivalent circuit using curve fitting from admittance values calculated from the measured S-parameters at frequencies from 1 MHz to 100 MHz. A typical equivalent circuit deduced is shown in Fig. 3. The elements C_1 and R_1 are mainly related to the electrical properties of the vacuole of the plant cell and are related to the real part of the complex permittivity ε' and the imaginary part of the complex permittivity ε'', respectively. The electrical loss factor is therefore defined by $\tan\delta = 1/(\omega C_1 R_1) = \varepsilon''/\varepsilon'$. The element C_2 is added to the equivalent circuit of specific root vegetables such as potatoes and pumpkins. Since the equivalent circuit was composed of four sub-circuits of Y_1, Y_2, Y_3, and Y_4, the electrical property of the equivalent circuit was analyzed using the admittance Y [Ω^-]. The reflection coefficient S_{11} of the S-parameter is calculated by $20\log(V_r/V_{in})$ using the reflective voltage V_r and the input voltage V_{in}. The admittance $Y_{in}(Z_0)$ defined at the input port of the VNA with measurement characteristic impedance Z_0 is shown in (1). The admittance Y_{in} of the equivalent circuit shown in Fig. 3 is calculated from (1) to (3), where G is the conductance, and B is the susceptance.

$$Y_{in}(Z_0) = (1 - S_{11})/(Z_0(1 + S_{11})) \quad (1)$$

$$Y_1 = -\mathrm{j}/\omega C_1, \quad Y_2 = 1/R_1 - \mathrm{j}/\omega C_2 \quad (2)$$

$$Y_n = 1/(R_n - \mathrm{j}/(\omega C_n)), \quad n \geq 3 \quad (3)$$

$$Y_{in} = 1/(R_5 + 1/(Y_1 + Y_2 + Y_3 + Y_4)) = G + \mathrm{j}B \quad (4)$$

III. CIRCUIT ELEMENT VALUES DEDUCED FROM ADMITTANCE VALUES PLOTTED ON THE SMITH CHART

We measured the S-parameters for four fruit samples, kiwi, grape, pear, and apple. The number of measurement points on each sample was about ten, and a median value was taken from these ten measurement points for each sample. From the measured reflection coefficients S_{11} of the S-parameters, the admittance values were calculated and plotted on the admittance grid of the Smith chart, as shown in Fig.4. Although the characteristic impedance of the measurement setup (Fig. 1) was 50 Ω, the reference impedance Z_0 represented by $G = 1$ on the Smith chart was changed to 250 Ω because the impedance of the fruit was much higher than 50 Ω hence the values of the measured S-parameters were converted to these values as measured with the impedance of 250 Ω. The admittance curves were therefore plotted using the reference impedance Z_0 of 250 Ω to allow more accurate analysis, and the comparison between measured admittance curves was performed for the high-impedance fruit.

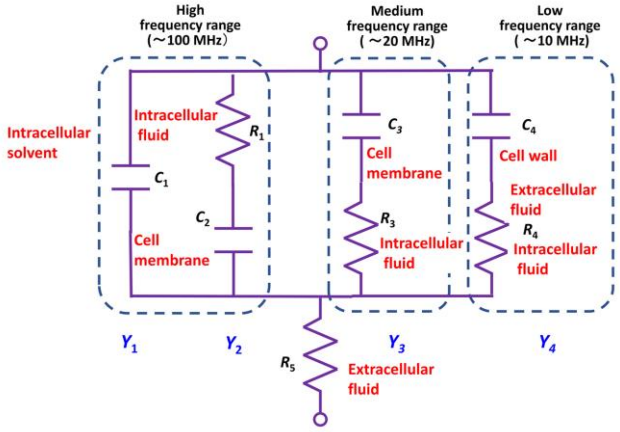

Fig. 3. Typical equivalent circuit of plant cell deduced from the S-parameter measurements.

IV. DEDUCED EQUIVALENT CIRCUIT ELEMENTS AND CALCULATED ADMITTANCE FOR FRUITS

The normalized value of G = 1(Z_0: 250 Ω) on the Smith chart is 0.004 [Ω^{-1}]. The values of seven circuit elements of the equivalent circuit (shown in Fig. 3) deduced from the admittance curves plotted for four fruit samples are summarised in Table I. When we calculate the admittances based on (3) and the equivalent circuit (Fig.3), the value of the characteristic impedance Z_0 was changed to the changed reference impedance Z_0, such as 250 Ω. The calculated and measured values are in good agreement, as shown in Fig. 4. It

should be noted that the equivalent circuit for the fruit does not include the circuit element of C_2. Since the circuit element of R_1 is mainly related to the conductance G of the admittance Y, the value of R_1 decreases with increasing the admittance Y_3. There is no significant difference in the values of the circuit element C_1 between the four fruits. Since the value of C_4 is larger than that of C_3 for each fruit, the circuit element C_4 may reflect the larger dielectric constant of the cellulose, which is a material of the plant cell wall.

TABLE I. EQUIVALENT CIRCUIT ELEMENT VALUES DEDUCED FROM THE REFLECTION COEFFICIENT S_{11} OF THE S-PARAMETERS MEASURED FOR FOUR FRUITS.

Circuit element	Kiwi	Grape	Pear	Apple	Unit
C_1	13	11.6	10	7.5	pF
R_1	292	422	643	690	Ω
C_3	23	15	10	2	pF
R_3	806	1230	2126	4370	Ω
C_4	557	360	218	35	pF
R_4	359	610	927	2970	Ω
R_5	10	9	10	3	Ω

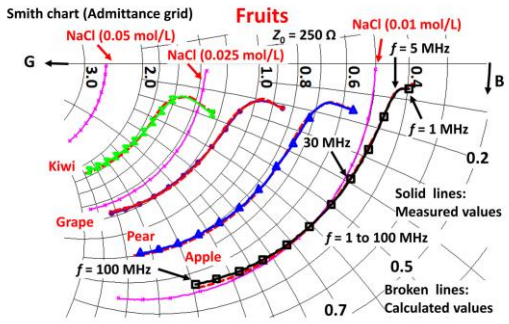

Fig. 4. Measured admittance and calculated curves plotted on the admittance grid normalized to Z_0 = 250 Ω of the Smith chart for four fruit samples.

A relationship between the change in admittance and the value of the equivalent circuit element is usually determined, as in the case of the persimmon as shown in Fig. 5. Two parts of Part-L and Part-H, divided at a point on the curve, represent admittance values measured at frequencies lower and higher than about 10 MHz, respectively. The subcircuits *Y3* and *Y4* are mainly related to the admittance curve of Part-L and consist of serial networks composed of C_n and R_n. The subcircuits Y_1 and Y_2 are related to the admittance curve of Part-H and consist of the circuit elements of C_1 and R_1.

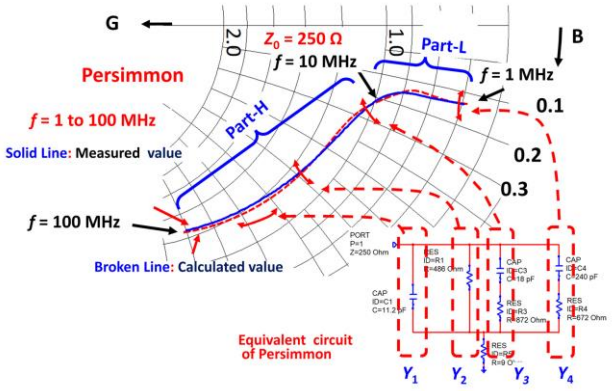

Fig. 5. Relationship between equivalent circuit elements and admittance values measured for a persimmon fruit.

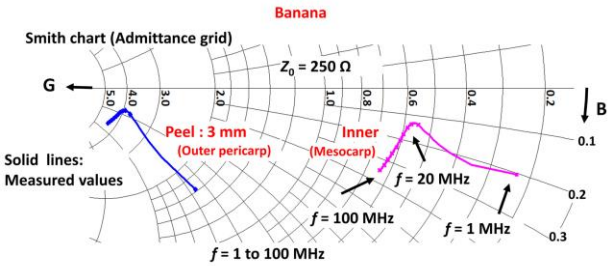

Fig. 6. The difference in measured admittance values between two parts of the peel (outer pericarp) and the inner portion (mesocarp) of a banana.

To compare the admittance values measured for the four fruit samples with that of a standardized material such as NaCl solution, admittance curves of NaCl solutions measured with three different molar concentrations of 0.05, 0.025, and 0.01 [mol/L] are also plotted. The S-parameters of these NaCl solutions were measured using the same measurement setup as used for the measurements with the four fruit samples [24]. Since the solution of NaCl consists of dissolved ions of Na^+ and Cl^- and the solvent of pure water H_2O, its electrical conduction is caused by the drift of these ions and the rotation and vibration of the polar molecules of H_2O. Since the equivalent circuit of the NaCl solution consists of a parallel network of C_1 and R_1, these elements and the admittance can be deduced from the measurements of S_{11} [24]. The admittance measured for apple was similar to that of the NaCl solution with a molar concentration of 0.01 mol/L at frequencies higher than approximately 30 MHz. It means that the parallel network of C_1 and R_1 of the fruit equivalent circuit represents an ionic solution such as the solution of NaCl. These elements of C_1 and R_1 relate the susceptance B and the conductance G, respectively. The banana consists of two parts of the peel (outer pericarp) and the inner part (mesocarp). The value of admittance of the peel was larger value than that of the inner part. And the length of Part-L of the admittance curve was much longer than that of Part-H for both parts, as shown in Fig. 6. The measured admittance value of the unpeeled banana is close to that of the peel because the length of the three pins of the SMA probe was 4 mm and the thickness of the peel was about 3 mm. Although the admittance value measured with the inner portion (mesocarp)

decreased, the length of Patr-L of the admittance curve was much longer than that of other fruits. Therefore, the banana cannot simply be classified as a fruit based on its electrical properties. To investigate the electrical properties of the decomposed plant tissue, a sample of apples was grated into fine pieces and separated into liquid and solid portions. As the size of the plant cell is generally 200 μm to 200 μm, the solid portion was removed using a 20μm-paper-filter, and then the S-parameters of the sample were measured. The 20μm-filtered sample showed admittance values larger than that of the untreated apple, and the admittance curve of Part-L was eliminated, as shown in Fig. 7. When the apple was grated, the plant cell wall and the membrane were destroyed and removed. Therefore, the part of Part-L and the sub-circuits Y_3 and Y_4 of the equivalent circuit are related to the plant cell membrane and wall.

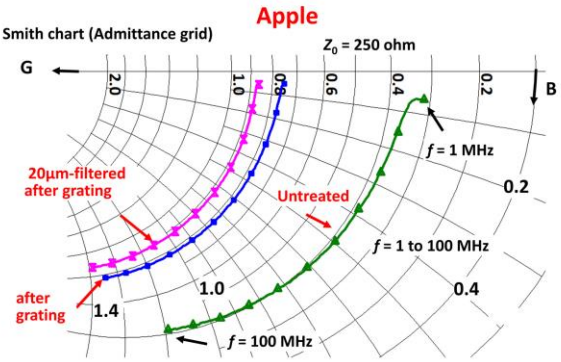

Fig. 7. Admittance values measured on untreated, grated, and 20um-filtered samples of an apple.

V. ADMITTANCE VALUES AND CIRCUIT ELEMENTS DEDUCED FOR VEGETABLES

We measured and calculated the admittance values using the equivalent circuits (Fig 3) and Table II for vegetables of ginger, potato, zucchini (courgette), pumpkin, and eggplant (aubergine), and the results are shown in Fig. 8. The measured and calculated values are in good agreement. The admittance values are higher, and the admittance curves have parts of Part-L longer than those of the fruits. It was confirmed that the parts of Part-L were eliminated after grating and filtering. The equivalent circuits for these five vegetables were deduced from the measured admittance values, and the values of the circuit elements obtained are summarized in Table II. A circuit element C_2 is added to the R_1 network for potato, sweet potato, and pumpkin because the conductance G of these plants varies with frequency, which is related to the imaginary part of the complex permittivity. There is no significant difference in the values of C_1 and R_1 between fruits and vegetables, but the values of C_3 and C_4 are larger, and the values of R_3 and R_4 are smaller than those of the fruits. Since the value of C_4 is larger than that of C_3 for each vegetable, the element C_4 may reflect the larger dielectric constant of cellulose, a material of plant cell walls. Therefore, it is assumed that there is a difference in the electrical configuration of the plant cell membrane and wall between vegetables and fruits.

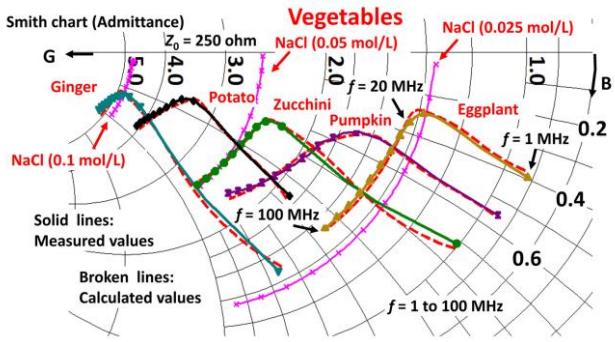

Fig. 8. Admittance values measured and calculated for five vegetables.

TABLE II. EQUIVALENT CIRCUIT ELEMENT VALUES DEDUCED FROM REFLECTION COEFFICIENT S_{11} OF S-PARAMETERS MEASURED FOR SIX VEGETABLES.

Circuit element	Ginger	Potato	Sweet potato	Zucchini	Pumpkin	Eggplant	Unit
C_1	13.5	12.5	16.5	14.5	13.5	8	pF
R_1	360	298	361	475	452	443	Ω
C_2	-	14	52.5	-	17	-	pF
C_3	74	323	60	1 61	208	31	pF
R_3	195	161	195	315	303	856	Ω
C_4	1155	3048	6696	656	1794	506	pF
R_4	77.5	117	368	170	246	352	Ω
R_5	2	8	41	12	21	12	Ω

We have measured and calculated significant changes in the admittance values after 20μm-filtring after grating for two root vegetables of potato and sweet potato, as shown in Fig. 9. These two samples showed a typical feature of the admittance curves of the root vegetables, as the length of Part-L was much longer than that of the Part-H. After 20μm-filtering after grating, the admittance curve of Part-L was eliminated. The plant cell wall and membranes were destroyed when the samples were grated. Hence most of the electrical signal paths through these parts in the lower frequency range were also eliminated.

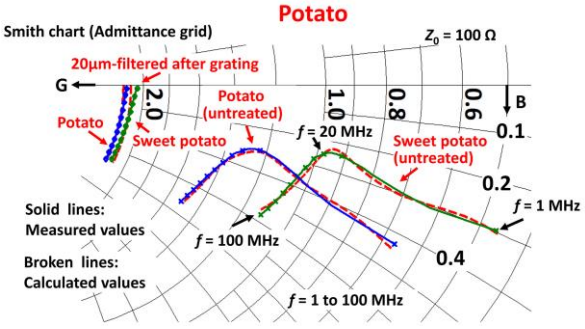

Fig. 9. Change in measured and calculated admittance values between 20 um-filtered and untreated root vegetables samples.

VI. CHANGE IN ADMITTANCE AFTER 20μM-FILTERING FOR RADISH

Radish (Japanese white radish) showed a particular characteristic of change in admittance that was quite different from that of the other vegetables. The admittance measured after 20μm-filtering after grating decreased, as shown in Fig. 10. However, one day later, the admittance conversely increased, and two days later, the admittance increased even more. The deduced values of the equivalent circuit elements after grating and filtering for the radish are shown in Table III. The circuit elements other than C_1 and R_1 were eliminated after the grating and filtering. Hence the deduced equivalent circuit became a parallel circuit C_1 and R_1. It was assumed that

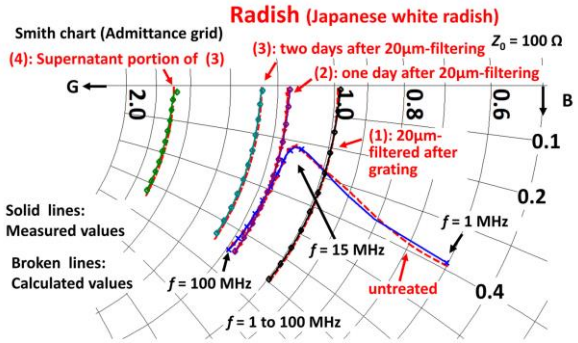

Fig. 10. Admittance values measured in four treatments for Japanese white radish.

when the radish was grated, its plant cells were destroyed, and a large number of enzymes were released in the plant- cells, thus causing oxidation to take place. When the polyphenols in the radish encounter oxygen, they are oxidized and create polyphenol oxidase (PPO, a family of enzymes), which then polymerizes further. Thus it decreased the value of admittance. One day and two days later, the filtered solution was separated into two portions, and the supernatant portion showed a high admittance. On the other hand, hot-white-radish (Japanese Karami daikon) and turnip did not decrease the admittance after 20μm-filtering after grating. Therefore, it is assumed that the decrease in the admittance after filtering after grating observed in the treated Japanese white radish was a unique characteristic caused by polyphenol oxidization.

TABLE III. THE ADMITTANCE VALUES DEDUCED IN FOUR TREATMENTS FOR JAPANESE WHITE RADISH.

Circuit element	Untreated	after 20μm filtering				Unit
		0 hour	1 day	2 days	Supernatant	
C_1	14.2	11	11	11	11	pF
R_1	411	101	86	79	59	Ω
C_3	94	-	-	-	-	pF
R_3	338	-	-	-	-	Ω
C_4	1155	-	-	-	-	pF
R_4	134	-	-	-	-	Ω
R_5	10.2	-	-	-	-	Ω

VII. ANALYSIS OF S_{21} MEASURED ON FRUIT AND VEGETABLES

We measured the transmission coefficients S_{21} of the S-parameters of fruit and vegetable samples using the same setup as used for the measurements of S_{11} (Fig. 1). The transmission coefficients S_{21} measured represent the electrical conductivity between two coaxial probes inserted at two different points in the sample. The distance between the two points was about 5 cm. The transmission coefficients S_{21} were measured at about ten paired points for each sample, and a median value of the measured values was calculated. The values of S_{21} for fruit and vegetables are shown in Fig. 11 and Fig. 12, respectively. There was a clear difference in the values of S_{21} between the twelve fruit and vegetable samples. For the four fruit samples, the measured values of S_{21} were relatively small, and the plotted values increased with increasing frequency. It is assumed that the electrical conductance through the polar molecules was dominant in the higher frequency range for the four fruit samples. For the eight vegetables, the values of S_{21} were relatively large, and the plotted values were mostly constant or decreased with increasing frequency. It is assumed that the electrical conductance through ionic material was dominant in the lower frequency range for the vegetables. The values of S_{21} measured with two samples of kiwi and banana are plotted with broken lines as shown in Fig. 12 and show a similar change in transmission coefficient S_{21} to that of the vegetable. Therefore, the two fruits of kiwi and banana can be classified as vegetables according to the result of the frequency dependence of the measured transmission coefficients S_{21}.

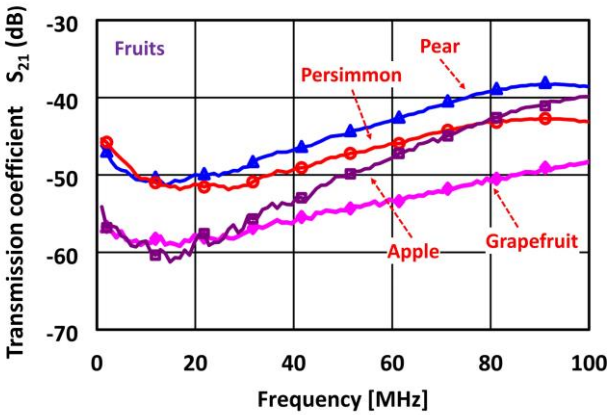

Fig. 11. Change in transmission coefficient S_{21} with increasing frequency from 1 MHz to 100 MHz for four fruits.

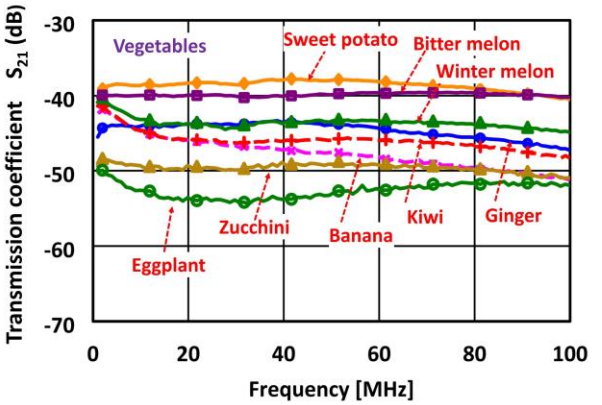

Fig. 12. Change in transmission coefficient S_{21} with increasing frequency from 1 MHz to 100 MHz for eight vegetables.

VIII. CLASSIFICATION OF FRUIT AND VEGETABLES

We classified 30 plant samples into two categories of fruit and vegetables based on four criteria deduced from the RF analysis: the characteristic of the admittance curves, the magnitude of the conductance, the change in the transmission coefficient, and the value of the circuit element. The thirty samples were therefore classified according to the specific four criteria: (a) the difference in the length between Part- L and Part-H of the admittance curve, (b) the magnitude of the conductance G compared to 1.4 ($5.6\times10^{-3}(\Omega^{-1})$), (c) the change in the value of S_{21} with increasing frequency, and (d) the value of 500 pF of the capacitance C_4. The classification result is shown in Fig. 13. Since there was no apparent difference in the measurement results for the four samples of acorn, banana, kiwi, and onion, these samples were classified as fruits and vegetables.

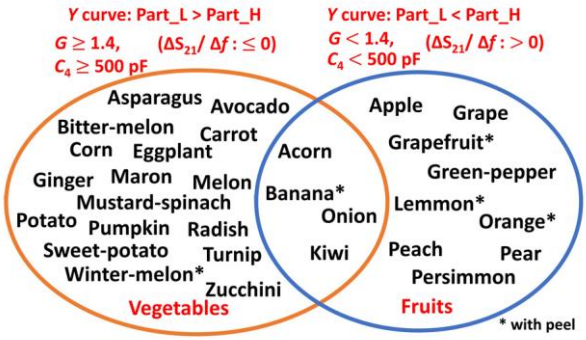

Fig. 13. Thirty fruit and vegetable samples classified according to four criteria deduced from the RF analysis.

IV. CONCLUSION

We deduced equivalent circuits of fruits and vegetables from the S_{11} of the S-parameters measured at frequencies from 1 MHz to 100 MHz using an RF signal measurement system configured with a portable VNA and tiny three-pin coaxial SMA probes. The deduced equivalent circuit consisted of four sub-circuits. Since the impedance of the fruits and vegetables is generally higher than a standard impedance of 50 Ω, the measured and simulated values were recalculated based on a reference impedance of *2*50 Ω or 100 Ω. We analyzed the admittance curves for four fruits and five vegetables and confirmed that the measured and calculated values mostly agreed. The admittance curve measured with each fruit and vegetable sample was divided into Part-L and Part-H for lower and higher frequencies, respectively. The length of Part-L of the fruit was shorter than that of the vegetables. Since the part of Part-L was related to two sub-circuits, Y_3 and Y_4, the electrical conductance at lower frequencies than about 30 MHz was mainly performed by large capacitance and low resistance related to the plant cell membrane and wall. We decomposed the plant cell wall and membrane to investigate this assumption by grating and filtering the fruit samples. We confirmed that the filtered samples showed increased admittance and that the admittance curves of Part-L were eliminated. We measured the transmission coefficients S_{21} and found that the change in the values with increasing frequency was positive for the fruits and mostly constant or negative for the vegetables. We classified 30 fruit and vegetable samples according to the four criteria deduced from the RF analysis. Since the SMA probe is tiny, it causes little or no damage to the samples in the measurement, making it possible to evaluate the electrical properties of fruit and vegetables during their growth in situ. This research method can be applied to other plant tissues and bio-tissue for analysis.

REFERENCES

[1] R. Raj, N.B.C. Bio, "Impedance Spectroscopy for the Assessment of Quality of Fruits by Constructing the Equivalent Circuit." *Int. J. of Eng. Res. and Tech*., 2, pp. 1773-1776, 2013.

[2] D.E. Khaled, N. Novas, J.A. Gazquez, R.M. Garcia, F. Manzano-Agugliaro, "Fruit and Vegetable Quality Assessment via Dielectric Sensing," *Sensors*, 15, pp. 15363-15397, 2015

[3] S. Sruthi, R. Dhavse, J.N. Sarvaiya, "Quality Assessment of Fruits and Vegetables using Bio-impedance based Expert System," *IJITEE*., 9, pp. 965-970, 2020.

[4] J.C. Caicedo-Eraso, F.O. Diaz-Arango, A. Osorio-Alturo, "Electrical impedance spectroscopy applied to quality control in the food industry," *C. Tech. Agropec.*, 21, pp. 1-19, 2020.

[5] J.N. Ikediala, J. Tang, S.R. Drake, L.G. Neven, "Dielectric Properties of Apple Cultivars," *Trans. of the ASAE*., 43, pp. 1175-1184, 2000.

[6] P.J. Jackson, F.R. Harker, "Apple Bruise Detection by Electrical Impedance Measurement," *Hortsci*., 35, pp. 104-107, 2000.

[7] W. Guo, S.O. Nelson, S. Trabelsi, S.J. Kays, "10-1800-MHz dielectric properties of fresh apples during storage," *J. of Food Eng*., 83, pp. 562-569, 2007.

[8] E. Vozáry, P. Benkó, "Non-destructive determination of impedance spectrum of fruit flesh under the skin," *J. Phys.: Int. Conf. on Elec. Bio-imped*., 224, pp. 1-4, 2010.

[9] W. Guo, X. Zhu, S.O. Nelson., R. Yue, H. Liu, Y. Liu, "Maturity effects on dielectric properties of apples from 10 to 4500 MHz," *LWT-Food Sci. and Tech*., 44, pp. 224-230, 2011.

[10] D. Jamaludin, S.A. Aziz, N.U.A. Ibrahim, "Dielectric Based Sensing System for Banana Ripeness Assessment," *Itn. J. of Envi. Sci. and Devel*., 5, pp. 286-289, 2014.

[11] M. Kafarski, A. Wilczek, A. Szypowska, A. Lewandowski,P. Pieczywek, G. Janik, W. Skierucha, "Evaluation of Apple Maturity with Two Types of Dielectric Probes," *Sensors*, 18, pp. 1-13, 2018.

[12] P. Ibba, A. Falco, B.D. Abera, G. Cantarella, L. Petti, P. Lugli, "Bio-impedance and circuit parameters: An analysis for tracking fruit Ripening," *Postharvest Biol. and Tech.*, 159, 2020.

[13] C.S. Widodo, D.R. Santosa, W. Sugianto, A.Y.P.Wardoyo, "A Study on electrical Impedance in Ripening Abon-bananas (Musa Paradisiaca Var. Sapientum) Process Stimulated by Ethrel (2-Chroroethyl Phosphonic Acid)," *Intl. J. of Geom.*, 18, pp. 39-44, 2020.

[14] E. Serrano-Pallicer, M. Munoz-Albero, C. Perez-Fuster,R.M. Peris, N. Laguarda-Miro, "Early Detection of Freeze Damage in Navelate Oranges with Electrochemical Impedance Spectroscopy," *Sensors*, 18, pp. 1-10, 2018.

[15] A.F. Neto, E.R. Cordeiro, N.C. Olivier, L.B. Marinho,D.Y.N. Morais, H.P.D. Oliveira, "Evaluation of the Pa-paya's maturation degree by electrical impedance," *African J. of Agric. Res.*, 14, pp. 1239-1246, 2019.

[16] R.N. Setiadi, L. Umar, "Fruit Sweetness Characterization Using Impedance Spectroscopy Method," *SPEK.: J. Fisik. dan Appl*., 4, pp. 81-88, 2019.

[17] M.S.A. Jumadi, D. Jamaludin, "Non-destructive Measurement of Rock Melon Fruit Properties using Electrical Impedance Spectroscopy (EIS) Technique," *ASM Sci. J.*, 13, pp. 20-26, 2018.

[18] J. Li, Y. Xu, W. Zhu, X. Wei, H. Sun, "Maturity assessment of tomato fruit based on electrical impedance," *Int. J. Agric. Biol. Eng*., 12, pp. 154-161, 2019.

[19] J. Peng, J. Tang, Y. Jiao, S.G. Bohnet, D.M. Barrett, "Dielectric properties of tomatoes assisting in the development of microwave pasteurization and sterilization processes," *LWT- Food Sci. and Tech*., 54, pp. 367-376, 2013.

[20] T. Hayashi, S. Todoroki, K. Otobe, J. Sugiyama, "Applicability of Impedance Measuring Method to the Detection of Irradiation Treatment of Potatoes," *Food Sci.Tech. Res*.,140, pp. 378-384, 1993.

[21] J. Chen, K. Pitchai, S. Birla, R. Gonzalez, D. Jones, J. Subbiah, "Temperature-dependent Dielectric and Thermal Properties of Whey

Protein Gel and Mashed Potato," *Trans. of the ASABE*., 56, pp.1457-1467, 2013.
[22] A. Kertesz, Z. Hlavacova, E. Vozary, L. Staronova, "Relationship between moisture content and electrical impedance of carrot slices during drying," *Int. Agrophys*., 29, pp. 61-66, 2015.
[23] M. Govindasamy, V. Mani, S. Chen, T. Chen, A.K. Sundramoorthy, "Methyl parathion detection in vegetables and fruits using silver@graphene nanoribbons anocomposite modified screen printed electrode," *Sci. Rpt*., 7, pp.1-11, 2017.
[24] K. Chinen, S. Nakamoto, I. Kinjo, "Two-port Equivalent Circuit Deduced from S-parameter Measurements of NaCl Solutions," *IETE Journal of Research*, IF 1.877, pp. 1-9, 2022.
[25] NanoVNA-manual, https://cho45. github.io /NanoVNA-manual, 2021.
[26] Microwave-office, https://www.awr.com /awr-software/ products/microwave-office, 2023.